Article

Not peer-reviewed version

Antimicrobial Properties of Polyester/Copper Nanocomposites by Melt-Spinning and Melt-Blowing Techniques

Alain Sánchez-González , Ricardo Rosas-Macías , José E. Hernández-Bautista , Janett A. Valdez-Garza , Nayeli Rodríguez-Fuentes , Florentino Soriano-Corral , Antonio S. Ledezma-Pérez , Carlos A. Ávila-Orta * , Víctor J. Cruz-Delgado *

Posted Date: 6 November 2023

doi: 10.20944/preprints202311.0279.v1

Keywords: Antimicrobial Properties; Nanocomposites; Copper; Melt Blowing; Melt Spinning; Textiles; Personal Protective Equipment

Article

Antimicrobial Properties of Polyester/Copper Nanocomposites by Melt-Spinning and Melt-Blowing Techniques

Alain Sánchez-González [1], Ricardo Rosas-Macías [1], José E. Hernández-Bautista [1], Janett A. Valdez-Garza [1], Nayeli Rodríguez-Fuentes [2], Florentino Soriano-Corral [3], Antonio S. Ledezma-Pérez [2], Carlos A. Ávila-Orta [2,*] and Víctor J. Cruz-Delgado [3,*]

[1] Departamento de Materiales Avanzados, Centro de Investigación en Química Aplicada, Saltillo, Coahuila. 25294, México; janett.valdez@ciqa.edu.mx, antonio.ledezma@ciqa.edu.mx, carlos.avila@ciqa.edu.mx
[2] CONAHCYT – Unidad de Materiales, Centro de Investigación Científica de Yucatán, A.C, Mérida, Yucatán. 97205, México; nayeli.rodriguez@cicy.mx
[3] Departamento de Procesos de Transformación, Centro de Investigación en Química Aplicada, Saltillo, Coahuila. 25294, México; florentino.soriano@ciqa.edu.mx, victor.cruz@ciqa.edu.mx
* Correspondence: carlos.avila@ciqa.edu.mx (CAAO), victor.cruz@ciqa.edu.mx (VJCD); Tel.: (+52 844 4983890 Ext. 1391 (CAAO))

Abstract: With the growing demand for personal protective equipment (PPE) in the face of the pandemic events caused by SARS-COV-2, the opportunity arises for the development of materials with characteristics such as antimicrobial, antiviral, antifungal activity, etc. The use of polymeric nanocomposites based on polyester/copper offers an alternative of great interest due to the versatility of the raw material and the high efficiency of copper as an antimicrobial additive. In this study, textile fibers prototypes with different Cu nanoparticles (CuNP) content were produced using melt-spinning to obtain bi-component multifilament fibers, and melt-blowing to obtain non-woven fabrics. The prototypes were tested against different pathogenic microorganisms such as *S. aureus*, *E. coli*, and *C. albicans*. It was shown that bi-component fibers offer more excellent protection against pathogens, while non-woven fabric only shows activity against *E. coli*. It was possible to identify that the CuNP were confined exclusively in the outer cover of the bi-component fibers, using different analytical techniques, which may be associated with the increase in antimicrobial activity, compared to the fibers present in the non-woven fabric, even when they present the same CuNP content.

Keywords: antimicrobial properties; nanocomposites; copper; melt blowing; melt spinning; textiles; personal protective equipment

1. Introduction

Hospital acquired infections (HAIs) have a tremendous economic and social impact nowadays, due to their elevated costs for health care and loss of jobs. In 2016, 7.2 to 14.9 billion U.S. dollars were spent on HAIs in the United States. Surgical site infections and infections with *Clostridioides difficile* accounted for 79% of the cost of HAIs [1]. The main microorganisms associated with HAIs are *Escherichia coli*, *Staphylococcus aureus*, *Enterococcus spp*, *Pseudomonas aeruginosa*, *Klebsiella spp*, and *Clostridioides difficile*, among others, meanwhile their prevalence along the time remains almost constant [2]. Sanitization of medical personnel is one of the main strategies to reduce the incidence of HAIs. Another strategy, is to provide effective and low-cost barriers that prevent the proliferation of pathogenic microorganisms in hospital environments such as in coatings for the walls and equipment surfaces, as well as clothing [3]. Reusable and disposable textile clothing is the front barrier for medical personnel where the incorporation of antimicrobial agents hinders the accumulation of pathogenic microorganisms, resulting in antimicrobial textiles.

 doi:10.20944/preprints202311.0279.v1

Tanasa et al., have identified 4 large groups of antimicrobial textiles. They were identified as textiles with (i) antimicrobial functionality, (ii) antimicrobial polysaccharides, (iii) antimicrobial metallic nanoparticles, and (iv) antimicrobial synthetic compounds [4]. However, considering their antimicrobial effectiveness and mechanism of action, as well as their toxicity *versus* tolerance, textiles with antimicrobial functionality can be divided into several classes [5] (i) biostats, biocides (antibacterial, antifungal, antiviral), barriers, and antibiofilm, (ii) textiles with bound or leaching antimicrobial finishing, (iii) textiles made of natural or synthetic fibers or blends, (iv) textiles able to release compounds with biological activity, and (v) wearables and washing resistant.

Of particular interests is the use of antimicrobial metallic nanoparticles such as silver (AgNP), gold (AuNP), and copper (CuNP), zinc (ZnNP), titanium (TiNP), and its oxides, as well as graphene to combat the most common and proliferating pathogens in hospital environments resulting in HAIs. These nanoparticles stand out due to the high levels of effectiveness shown even at very low concentrations [6–12]. Metallic nanoparticles can be incorporated or impregnate into fibers (either filaments of non-woven fabrics) to result in fibers with antimicrobial effect. Textile filaments from synthetic polymers such a polyester (usually poly ethylene terephthalate, PET) can be produced industrially by means of melt-spinning, while non-woven fabrics (NWF) of the same can be fabricated by means of melt-blowing. It well-know that other process can result in filaments and NWF, but they are out of the scope of this study.

Zhou et al., use a kind of Cu_2O and Cu_2O@ZrP micro-nano composite by loading Cu_2O onto ZrP nanoflakes, through an *in-situ* polymerization method, Cu2O@ZrP composite could be successfully and uniformly integrated into PET fibers, presenting highly enhanced mechanical properties and antibacterial activities against *E. coli*, *S. aureus*, and *C. albicans* were compared to its control sample obtained by the melt-blending method. In addition, the dispersion of nano-Cu2O@ZrP in the corresponding PET matrix fabricated were also compared and discussed in detail. The integration on Cu_2O and its nanohybrids by the *in-situ* polymerization method yield high antibacterial activity at low contents as 0.2 and 0.4% w/w. As is well known, Cu oxides possess higher antibacterial activity than their metallic counterparts, besides the integration in layered structure of ZrP enhance the dispersability in the fibers obtained [13].

Zhu et al., prepare an antimicrobial PET masterbatch using magnesium-based antimicrobial agent (MAA, MgO) as the functional material by melt blending, then a kind of antimicrobial fabric was prepared using PET masterbatch and pure PET resin by high-speed melt-spinning and weaving technology with contents of 1, 2, 3, 4, and 5% w/w of MAA. A series of techniques were used to characterize the fibers and fabrics, and the antimicrobial property of the fabrics was tasted against *E. coli*, *S. aureus*, *C. albicans* and *A. niger* using alive-microorganisms-counting method. Besides, the physico-mechanical properties of fabrics were also tested and the antimicrobial property after washing, found a very low diminish after 50 cycles [14].

Yeo and Jeong prepared continuous bi-component core-shell fibers by a melt-spinning method with polypropylene and silver nanoparticles. The melt-spun fibers were characterized using different techniques. The antibacterial effect was evaluated by AATCC 100 test. The results of the DSC thermograms and X-ray diffraction intensity pattern indicated that the crystallinity of polypropylene, including silver nanoparticles, decreased slightly compared with that of pure polypropylene fibers. SEM micrographs showed that the average diameter of the silver nanoparticles was approximately 30 nm, and some particles had aggregated. The fibers, which contained silver in the central part (core), did not show antibacterial effects. However, the fibers with silver added in the shell part showed excellent antibacterial effects against different bacteria using concentrations of 0.3 and 5% w/w [15].

Other studies have been dealing with polymer fibers containing metal nanoparticles. However, in these cases, the authors focused on processability and physical properties rather than antimicrobial properties. Guerra et al., prepared potential antimicrobial PET-AgNP nanocomposite filaments for textile applications, incorporating AgNP in a PET matrix at different concentrations by extruding the PET resin with specific amounts of a 10% (w/w) AgNP/PET masterbatch. Then, rheological characterization was carried out, and filaments were produced for mechanical, optical, and thermal analyses. The incorporation of up to 0.20% (w/w) of AgNP in the polymeric matrix has not

 doi:10.20944/preprints202311.0279.v1

significantly altered the overall properties of PET nanocomposites. Beyond this quantity, the processability of the polymeric nanocomposite for forming filaments is compromised [16]. Meanwhile, Guzman et al., described the preparation and characterization of a bactericidal synthetic fiber composed of recycled polyethylene terephthalate (rPET) and CuNP through an extrusion process using triethylene glycol as a solvent, which allowed the mixture to be fluidized through the extruder. The study of the degree of dispersion of the nanoparticles in the PET matrix has been carried out using X-ray diffraction and scanning electron microscopy. X-ray Fluorescence was used to demonstrate the presence of copper in the polymer matrix of the fiber. At the same time, the mechanical properties of the obtained fiber were evaluated [17].

On the other hand, non-woven fabrics have found a large number of applications due to their intrinsic properties like: filtration, absorbency/repellent, antimicrobial/antiviral, lightweight, pore size control, thermal/acoustic insulation, among others. However, some of these properties require additives that are usually applied externally or on the finished product, with the purpose of reducing the additive content use. The need to wear a face mask in public spaces was implemented during the 2019 coronavirus pandemic with the aim of lowering infections between population. Different approaches were tested to increase the effectiveness of these products from a scientific and industrial point of view.

One study by Abazari et al. aimed to impregnate the masks with silver nanoparticles through a sonochemical treatment. Therefore, the polypropylene NWF substrates were treated at different sonication times and AgNP concentrations. Different parameters were evaluated in the treated masks, such as AgNP release, filtration efficiency, pressure drop, electrical conductivity, as well as antibacterial activity against *E. coli* and *S. aureus*. The results showed that by using longer sonication times and concentrations of the AgNP precursor, a more significant and more stable coating and high antibacterial activity were obtained without sacrificing cytotoxicity towards *Artemia nauplii* cell lines. The above suggests its potential application for protection masks against different pathogenic entities [18]. In another work by Ferreira et al., different polypropylene NWFs were characterized in terms of their structural, physicochemical, and comfort-related properties to obtain 3-layer masks. The NWF selected for the interlayer was functionalized with 0.3 and 1.2% w/w of zinc oxide nanoparticles (ZnO NPs) using three different methods. Functionalized fabrics obtained by dry pad immersion revealed the most promising data, with 0.017 ± 0.013% w/w ZnO NP located mainly on the fiber surface and capable of completely eradicating *S. aureus* and *E. coli* colonies within 24 h tested (ISO 22196) in addition to contributing to the inhibition of the growth of a substitute for the SARS-CoV-2 virus (ISO 18184 standard). The developed three-layer, multi-scale fibrous structures with antimicrobial capabilities have immense potential as functional protective masks [19]. The applications of silver, copper, and zinc ions and metallic particles of Cu, Ti, and Zn oxides have been found to be useful antimicrobial reagents for the bio-functionalization of various materials and their surfaces. In this sense, aqueous dispersion of synthetic copolymers based on acrylic and these nanoparticles were used to modify the surface of NWF of polyester and polylactic acid (PLA). The antimicrobial (antibacterial and antifungal) properties of textile materials (fabrics and non-wovens) functionalized with the above-mentioned active agents exhibiting antimicrobial properties ($CuSiO_3$, TiO_2, ZnO, or $ZnO{\cdot}SiO_2$) were highly dependent on the content of the agents in water dispersions. These new functionalized non-woven polymeric textile materials can find practical applications in the manufacture of filters for hospital air conditioning systems and for the automotive industry, as well as in air purification devices [20]. Gabbay et al., by means of impregnation or coating with cationic copper, confer to cotton or polyester fibers a broad spectrum against bacteria, viruses, and fungus properties. This platform allows the mass production of woven and non-woven fabrics such as sheets, pillow covers, gowns, socks, and air filters, among others, without the need to alter any industrial procedures or machinery; only the introduction of copper oxide-treated fibers containing 3 – 10 % w/w. These authors point out that impregnated fibers do not interfere with the handling of end products, washing cycles, color changes, press, etc. At the same time, antimicrobial fabrics can alleviate athlete's foot or decrease bacterial colonization in a clinical setting; besides, they do not have skin-sensitizing or any adverse effects [21].

 doi:10.20944/preprints202311.0279.v1

In the present study, the behavior of polymeric nanocomposites based on CuNP and polyester is studied to determine their viability of being converted into a textile using two different techniques, such as melt-spinning and melt-blowing, to subsequently evaluate its structural, morphological, and antimicrobial properties against various pathogenic microorganisms, depending on the CuNP content and the method of obtaining the textile. The results obtained will determine whether these textiles can be used in the manufacture of personal protective equipment for medical personnel, hospital textiles, and air filters, among others, that help mitigate the proliferation of pathogens.

2. Materials and Methods

Commercial copper nanoparticles (CuNP) with a purity of 99.8%, an average diameter of 25 nm, and hemispherical geometry were used, according to data from the supplier SkySpring Nanomaterials (Houston, TX). The polyethylene terephthalate resin (PET) used was provided by Indorama Ventures Inc. company (Queretaro, Mexico), used in the injection molding process, with an intrinsic viscosity (IV) of 0.82 ± 0.02, melting temperature of 252 °C, and about 12% of solids. To avoid oxidation of CuNP, they were previously mixed with mineral oil in an inert nitrogen atmosphere and kept under mechanical stirring for 1 h. Subsequently, they were added to a determined amount of previously dried polyester resin and mixed uniformly to coat the resin pellets. This mixture of resin and CuNP was processed by melt mixing to obtain a masterbatch with a concentration of 1% by weight, as described below.

Masterbatch preparation (PET/1% CuNP). In order to obtain a uniform dispersion of 1 %w/w of CuNP in the polyester resin, the ultrasound-assisted melt extrusion (USME) technique was used, for which a Thermo Scientific twin-screw extruder model Prism TSE 24-MC (Karlsruhe, Germany) was used, which has a screw diameter of 24 mm, an L/D ratio 40:1, with 2 intensive mixing zones. A flat temperature profile of 260 °C was used. An accessory was attached to the extruder die to apply ultrasound waves of variable frequency between 15 – 50 kHz, with a power of 750 W, as described previously [22–24]. The material processed in this way was cooled, cut, and placed in an oven at 120 °C for 12 h to promote its recrystallization before being processed using melt-spinning and melt-blowing techniques.

Fibers preparation. The preparation of multifilament fibers and non-woven fabrics was carried out in a Multi-functional laboratory and pilot melt spinning systems from Fiber Extrusion Technology (Leeds, United Kingdom) using the FET-100 Extrusion, FET-101 Multifilament and FET-102 Nonwoven modules, which has two single-screw extruders with a screw diameter of 25 mm and 20 mm respectively, both with an L/D ratio of 30:1.

Multifilaments by melt-spinning. In this case, the two extruders were used. The purpose of performing co-extrusion is to obtain a fiber with a core-shell configuration and expose the CuNP on the surface of the fiber. To achieve this objective, neat polyester resin was fed into one extruder to form the core, and the PET/1% CuNP masterbatch was fed into the other extruder and mixed with more polyester resin to dilute its concentration until obtaining a final concentration of 0.1, 0.25 and 0.5% by weight, directly during the extrusion process. In both extruders, a temperature of 295 °C was used throughout the barrel, dosing pump, head, and spinneret. The multifilaments obtained were cooled with air and subjected to a stretching process using three pairs of rollers that operate at different temperatures (25, 90, and 110 °C) and speeds (100, 120, and 240 mpm), respectively. They were collected in the winder using a speed of 300 mpm to obtain a stretching ratio of 3:1. A circular spinneret with 18 holes with a diameter of 0.125 mm and a length of 1.4 mm was used.

Non-woven fabrics by melt-blowing. In this case, only the 25 mm extruder was used, where the PET/1% CuNP masterbatch was mixed with more polyester resin to dilute its concentration until obtaining a final concentration of 0.1, 0.25 and 0.5% w/w directly during the extrusion process. A temperature of 295 °C was used throughout the barrel, dosing pump, head, and spinneret. To stretch the filaments and form the non-woven fabric, an airflow of 1000 l/min was used at a temperature of 300 °C. The filaments were deposited on a conveyor belt advancing at a speed of 0.6 mpm and were finally collected in a winder on a cardboard core. A straight spinneret with 41 holes with a diameter of 0.250 mm and a length of 2.4 mm was used [25,26].

 doi:10.20944/preprints202311.0279.v1

Characterization. Differential scanning calorimetry (DSC) was used to determine the main transition temperatures of the PET and PET/CuNP master batch. A DSC Discovery Series 2500 equipment from TA Instruments (New Castle, DE), a heating/cooling rate of 10 °C/min was used, in a range of 10 – 300 °C, in addition to inert atmosphere with nitrogen gas with a flow of 50 ml/min. To determine the thermal stability of the material during the subsequent melt-spinning and melt-blowing processes, a thermogravimetric analyzer (TGA) model Q500 was used from TA Instruments (New Castle, DE); the analysis conditions were heating from 25 to 800 °C at a rate of 10 °C/min, a nitrogen flow of 50 ml/min and approximately 8 – 10 mg of each sample were used. The denier of the multifilaments was calculated according to the linear mass ratio (gr) of each 9000 meters of fiber obtained in the melt-spinning process. Likewise, the density of the NWF was determined in 10 x 10 cm samples; in both cases, an OHAUS Explorer (Newark, NJ) analytical balance was used with a resolution of 0.0001 g. The samples obtained through the melt-spinning and melt-blowing processes were observed through an Olympus BX53 optical microscope (Tokyo, Japan), which has a digital camera attached that allows the capture of images. The samples obtained were analyzed by scanning electron microscopy (SEM) in order to observe and corroborate the presence of CuNP on their surface by chemical analysis (EDS). The analysis of the samples was carried out in a field emission electron microscope JEOL model JSM-7401F (Tokyo, Japan). The operating conditions were 2.0 kV acceleration voltage and a working distance of 8 mm. The samples were previously coated with gold-palladium. Antimicrobial activity tests for multifilaments were carried out in accordance with the procedure described in JIS Z-2801 as described in [27–29]. Which consists of inoculating a culture medium with a strain of *S. aureus* and/or *E. coli*, subsequently placing a sample of filaments with different copper content, allowing the culture to incubate for 24 h at 37 °C and later, count colony forming units (CFU) to determine the percentage of inhibition of antimicrobial activity. In the case of non-woven fabrics, the agar diffusion tests were carried out using strains of *Staphylococcus aureus* (*S. aureus*), *Escherichia coli* (*E. coli*), and *Candida albicans* (*C. albicans*), during the procedure, the turbidity of the suspension was adjusted to the McFarland turbidity standard of 0.5. At this absorbance, the bacteria concentration is standardized to approximately 1.5 x 10^8 CFU/ml and is used as a working microbial solution to inoculate the culture medium. A portion of the different samples of approximately 1 x 1 cm was placed in the center of the culture medium.

3. Results

3.1. Masterbatch Characterization

3.1.1. Differential scanning calorimetry (DSC)

It is known that with the incorporation of nanoparticles in thermoplastic polymers, the main thermal transitions (glass transition (T_g), melting (T_m), crystallization (T_c)) can show variations with respect to the neat polymer. The above must be considered when these nanocomposites are transformed into a final product. Using DSC, it was possible to determine the melting behavior during heating fusion for the PET and PET/1% CuNP samples, which will be used as a masterbatch to obtain lower concentrations by dilution. Firstly, it is observed that the PET sample has a T_g of around 78 °C and a melting temperature T_m around 242 °C. In the case of the masterbatch, it exhibits a T_g around 80 °C, as well as a small endothermal transition around 138 °C (due to the mineral oil), while the melting temperature T_m increases to 250 °C, which indicates that the presence of CuNP shifts the melting of the material to higher temperatures (Figure 1A). The above may be due to the formation of crystals with greater perfection, which may have formed from CuNPs that are homogeneously dispersed and that act as nucleation agents.

During cooling (Figure 1B), it can be seen that the PET sample has a crystallization temperature T_c located at 152 °C and a T_g around 80 °C, which corresponds well to a neat polyester resin that does not contain additives and/or copolymers that prevent or delay crystallization. For its part, the PET/1% CuNP sample exhibits a notable increase in the crystallization temperature, with a shift towards higher temperatures, in addition to the formation of two crystalline populations at 207 and 195 °C,

Preprints (www.preprints.org) | NOT PEER-REVIEWED | Posted: 6 November 2023 doi:10.20944/preprints202311.0279.v1

respectively, as well as a T_g that is around 80 °C. The increase in T_c and the formation of two crystalline populations suggests, as indicated above, that CuNPs are homogeneously dispersed in the PET matrix, acting as nucleation agents, generating more homogeneous crystals that crystallize at higher temperatures, in addition to the presence of secondary crystals that can originate at the expense of the first ones. On the other hand, this behavior during crystallization is typical in polyester resins in the presence of small amounts of nucleating agents. The increase in crystallization temperature is a parameter that must be considered during the melt-spinning and melt-blowing processes to which the material obtained will be subjected, with the purpose of avoiding early solidification of the material in some areas of the extrusion process.

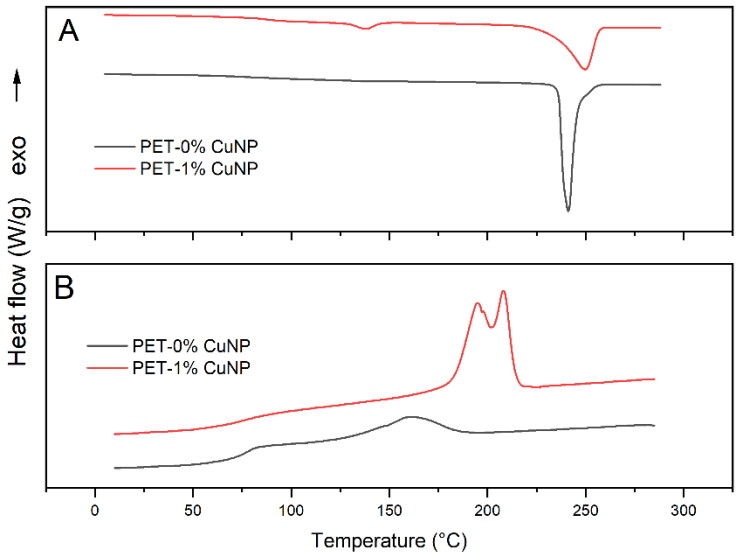

Figure 1. Behavior during DSC heating (A) and cooling (B) for PET and PET/CuNP samples.

Guerra et al., report the preparation of PET/Ag polymeric nanocomposites with different concentrations of Ag obtained by melt mixing and subsequent dilution from a masterbatch [16]. During the thermal analysis of the nanocomposites obtained, they reported similar values for the T_g, T_c, and T_m of the polymer with and without the addition of Ag nanoparticles, which is similar to the results obtained in this study. However, the increase in the T_m of the 1% (w/w) PET/CuNP sample suggests that the Cu nanoparticles are acting as nucleation agents. Mata-Padilla et al. prepared polymer nanocomposites by ultrasound-assisted melt extrusion based on PP/Cu with different Cu contents. Through thermal analysis and particularly during non-isothermal crystallization at different rates, it was observed that the presence of CuNP promotes an increase in the rate and temperature of crystallization as the content of copper nanoparticles increases [30]. Other reports in the literature suggest that the main thermal transitions in polymeric nanocomposites are modified, particularly the crystallization and melting temperatures, due to the presence of metallic nanoparticles because these can promote the nucleation of polymeric crystals on their surface by acting as nucleation agents, even in very low concentrations < 5% (w/w) [31–33].

3.1.2. Thermogravimetric Analysis (TGA)

In order to demonstrate whether the presence of CuNP promotes an increase or decrease in the thermal stability of the masterbatch prior to being processed using melt-spinning and melt-blowing techniques, a thermogravimetric study was carried out. The results are shown in Figure 2. It can be seen that as the temperature increases, the PET sample presents a single weight loss event that begins around 380 °C and ends at approximately 460 °C. With the addition of 1% (w/w) of CuNP, the sample also presents a single degradation event, which begins at slightly lower temperatures without evidencing any anomalous behavior. Based on this study, the polymeric nanocomposite can be

 doi:10.20944/preprints202311.0279.v1

considered to be thermally stable during the conditions required in melt-blowing and melt-spinning processes.

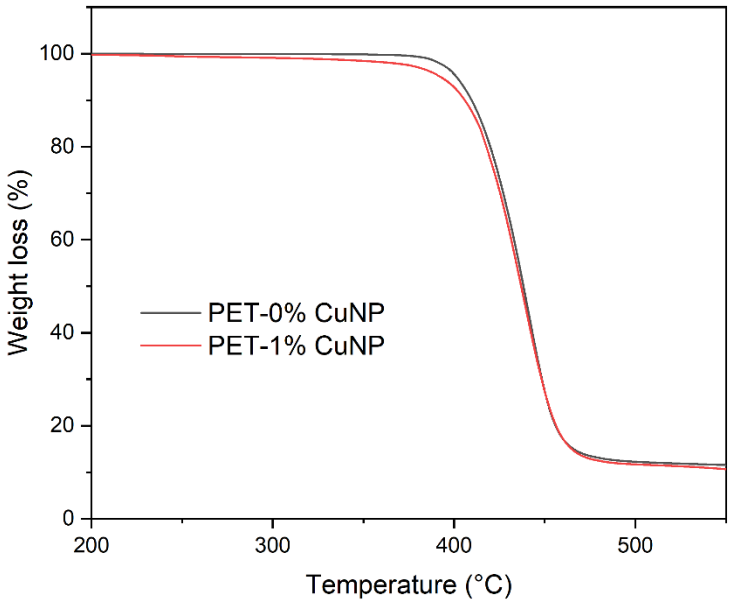

Figure 2. Thermal stability for the PET and PET/1% CuNP samples.

During the synthesis of PET and hybrids with Ag/TiO_2 nanoparticles, degradation was observed in a single step and within the same temperature range for the pure polymer, while the nanocomposite exhibits several weight loss events, the first occurring at a temperature of 253 °C equivalent to 9% by weight, subsequently at 420 °C a loss of 84% by weight was observed and is attributed to the thermal decomposition of PET derived from the byproducts present after the synthesis [34]. On the other hand, the addition of OMMT and/or SiO_2 in 0.5, 1, and 2 % (w/w) in PET promotes a single degradation event in the same interval of temperature that our sample [35].

Based on the previous results and taking into consideration that a dilution of the masterbatch will be carried out during the processing of the samples by melt-spinning and melt-blowing, it can be considered that the DSC and TGA techniques provide sufficient information regarding the profile temperature that should be used for processing the samples. Although it is important to consider the flow properties of the polyester based on the shear speed and/or the determination of the fluidity index, it is widely known that polyesters, polyamides, and other engineering polymers usually suffer a decrease in molecular weight after an extrusion cycle, which improves its fluidity and facilitates processing in a subsequent extrusion cycle.

3.2. Multifilament and NWF Characterization

Multifilament bi-component fibers produced by melt-spinning and NWF fabricated by means of melt-blowing were characterized by physical properties and morphology prior to their antimicrobial analysis.

3.2.1. Denier and grammage

Polyester fiber is the most important synthetic fiber in the world in terms of production due to its low cost, the ease with which it can be processed, and excellent performance. Among its properties, polyester is a strong fiber (4.5 g/den) [36]. The growing demand to increase the properties of previously known fibers and to create new fields of application of textile materials has been the cause of the rapid growth of microfiber technology and the increasing potential of the textile industry [37]. According to the calculations of total denier (TD) that corresponds to the lineal mass of 9000 m, expressed in g, a gradual increase in this parameter is observed as the Cu content increases, as shown

 doi:10.20944/preprints202311.0279.v1

in Table 1. Additionally, the denier per fiber (DPF) was calculated to obtain the individual linear mass of each fiber. On the other hand, the weight of the non-woven fabric was determined; this constitutes the weight per square meter, expressed as g/m² or gsm. This parameter is important when costing and defining the price since the weight will give the consumption ratio, depending on the final application [38]. Table 1 shows the grammage of the fabricated non-woven fabrics as a function of the concentration of CuNP. This value increase depending on the nanoparticles content. However, this increase is not significant compared to the increase in denier.

Table 1. Denier in multifilament fibers and grammage in NWF with different Cu content.

Sample	Multifilament		NWF
	Total Denier	DFP	gsm
PET	222	12.3	67.5
PET/0.10% CuNP	345	19.1	68.3
PET/0.25% CuNP	369	20.5	68.8
PET/0.50% CuNP	391	21.7	69.5

3.2.2. Multifilament Morphology

Fiber morphology. In order to demonstrate the formation of a core and shell in the bi-component multifilaments, several un-stretched filaments were placed in a sample holder, and a cross-section was made with the help of a sharp knife to avoid as much as possible deformation of the filament, the cut was carried out at room temperature, see Figure 3. As can be seen in Figure 3A, the cross-section of the filaments is circular. For this particular case, it is not possible to identify the border between the core and the shell because both sections are made of the same material, and there is no contrast between them. As the CuNP content increases, the formation of a halo or shell in each filament is observed, and this is better defined in Figure 3D, which corresponds to the highest CuNP content (0.5% w/w). It can also be seen that there is a heterogeneous distribution in the diameter of the filaments, being more uniform for Figure 3D. According to the information collected through this technique, it was determined that the proportion of the core/shell is an average 80:20. The diameter of the filaments is 17 ± 3 μm, at a draw ratio of 3:1. It is considered that after the drawing process, the proportion between the core/shell remains in a similar proportion, which would still confine more to the CuNPs in the shell of each filament since its thickness decreases proportionally [37,39,40].

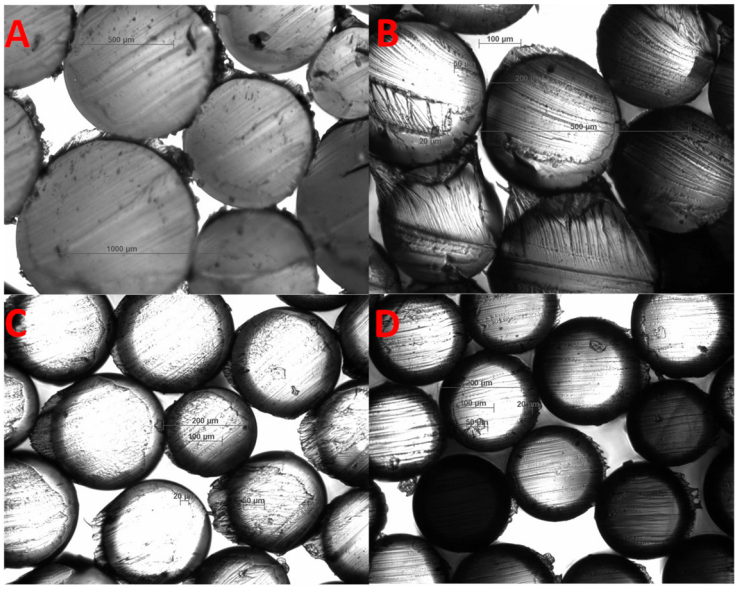

Figure 3. Optical microscopy images of multifilaments with core/shell morphology A)0%, B)0.1%, C)0.25%, and D)0.5% CuNP, at 10X.

Preprints (www.preprints.org) | NOT PEER-REVIEWED | Posted: 6 November 2023 doi:10.20944/preprints202311.0279.v1

Morphology and elemental analysis by SEM. To corroborate the presence of CuNP in the bi-component multifilament, elemental analysis was performed on different sections of the shell filament by means of SEM, as seen in Figure 4. Once again, the image corroborates the circular shape of the filaments. Figure 4A corresponds to the PET sample; the cryo-fracture of the filament shows good compatibility between core and shell, and no contrast or evidence of the concentric fiber is observed. Meanwhile, for PET/0.5 % CuNP (Figure 4B), it is not possible to identify the core and shell zones due to the excellent compatibility of both samples. Elemental analysis was implemented in two specific zones near the surface of the filament; their composition is shown in Figure 4C. In both zones, Cu signal appears, and their atomic content has a value very close to the theoretical content of 0.5 %; nevertheless, the weight content is higher, around 2.5 % w/w, which is five times greater than the theoretical amount. This quantity could be related to the confinement of the CuNP during the bi-component fiber forming, where the PET nanocomposite was placed in the shell of the filament [41].

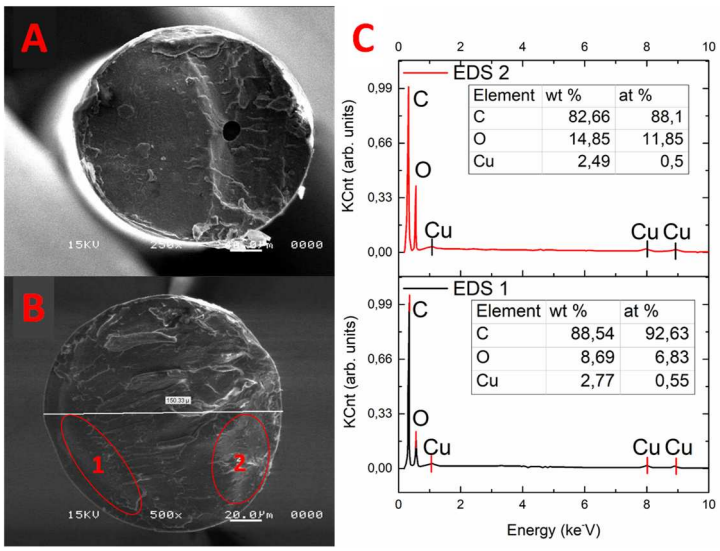

Figure 4. SEM image and elemental analysis of the core/shell sample with 0 and 0.5% w/w CuNP.

The dispersion of CuNP in the nanocomposites by scanning electron microscopy (SEM) and elemental analysis was performed in samples of PP/CuNP. The elemental analysis presents peaks associated with elemental copper, in addition to small traces of oxygen, suggesting partial oxidation of the particles upon contact with the environment [27].

On the other hand, the morphology of PP/CuO composites was analyzed by scanning electron microscopy. The size of the CuO particles was determined to be approximately less than 5 microns, and the aggregation of CuO could be formed due to their high surface energy caused by the size effect of the particles. Furthermore, a small amount is uniformly dispersed of the CuO and can be observed in the PP matrix. [37,42]. Zhou et al., showed similar results by SEM images of CuO@ZrP hybrids on the surface of PET fibers, besides to point out that the melt-blending or in situ polymerization processes would not destroy the structure of CuO@ZrP hybrids [13].

3.2.3. NWF Morphology

Fiber morphology. Through optical microscopy, it was possible to observe the morphology of the fibers that make up the non-woven fabric, the distribution of diameters, the intertwining between filaments, as well as a gradual change in color, see Figure 5. The morphology of the filaments is mostly rectilinear and free of protuberances, in addition to presenting high interlacing density. It can also be observed that as the concentration of CuNP increases, the color of the sample becomes darker and gives the appearance of having protuberances at the junction points of the filaments. Due to the low amount of magnification that this microscope has, it is not possible to identify the presence of CuNP in the multifilaments.

Preprints (www.preprints.org) | NOT PEER-REVIEWED | Posted: 6 November 2023 doi:10.20944/preprints202311.0279.v1

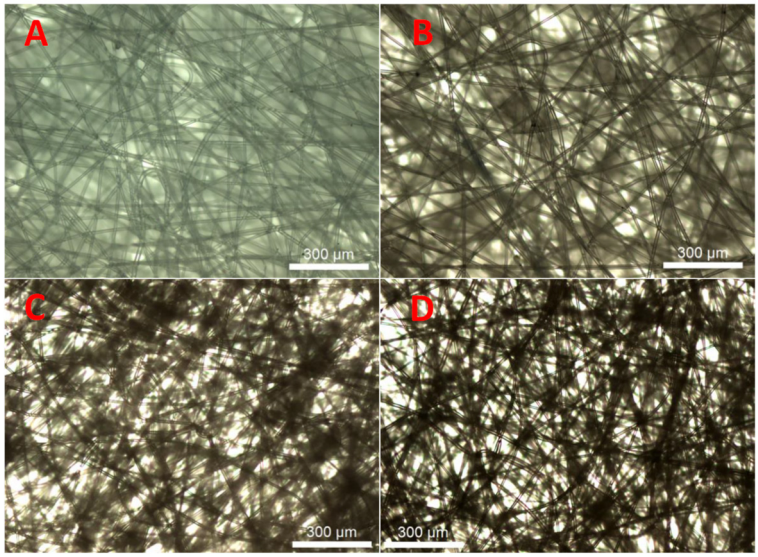

Figure 5. Optical microscopy images of non-woven fabrics A) 0%, B) 0.1%, C) 0.25%, and D) 0.5% CuNP at 20X.

In a study on samples of PET non-woven fabric with antimicrobial properties based on copper nanoparticles, the samples also present a change in color as several layers of the nanoparticles are deposited using plasma. At the same time, the structure of the non-woven fabric was not altered by the process [41]. The same behavior occurs during the preparation of copper nanocomposite textiles by magnetron sputter coatings [43].

Morphology and elemental analysis by SEM. Figure 6 shows images corresponding to NWF with 0.5% CuNP, with different magnifications. It can be seen in greater detail in Figure 6A that the fibers have an average diameter distribution of 8 ± 4 microns, which suggests that the diameters are quite uniform. Furthermore, it can be seen that the fibers have a cylindrical structure apparently free of defects and did not resemble a union between them, as described in the images observed by optical microscopy. In Figure 6B, the deposit of small particles of some contaminant, probably dust, with an average size between 1–3 microns can be seen, which should not be confused with CuNPs, which have lengths less than 100 nm. In Figure 6C, observed at 10,000X, clear spots begin to be seen on the surface of the fiber, which is separated and distributed over the entire surface, in addition to having sizes less than 1 micron, which is identified in the figure with a circle. In Figure 6D, observed at 30,000X, white dots with a semi-circular geometry and sizes less than 100 nm can be seen, which corresponds with the CuNPs that were introduced into the fibers and that are exposed on the surface (identified with a circle). In addition to seeing a groove that suggests the nanoparticle was dragged on the surface of the fiber, which could have happened during the stretching of the filaments when the sample was fabricated.

An elemental analysis was carried out on this sample to corroborate the presence of copper in the fiber. In Figure 6E, it can be seen that in addition to C and O, the other elements present are Cu and Ca, where Ca can come from catalysts and/or additives used in polyester synthesis, while the Cu content corresponds to 0.41% by weight, as seen in the Table in Figure 6, which agrees with the theoretical content of Cu that was added. Due to the NWF preparation method, it is considered that not all the Cu is exposed on the surface of each fiber and that a large part of it is dispersed inside the fiber. The above may have considerable repercussions in terms of the activity against different microorganisms.

Preprints (www.preprints.org) | NOT PEER-REVIEWED | Posted: 6 November 2023 doi:10.20944/preprints202311.0279.v1

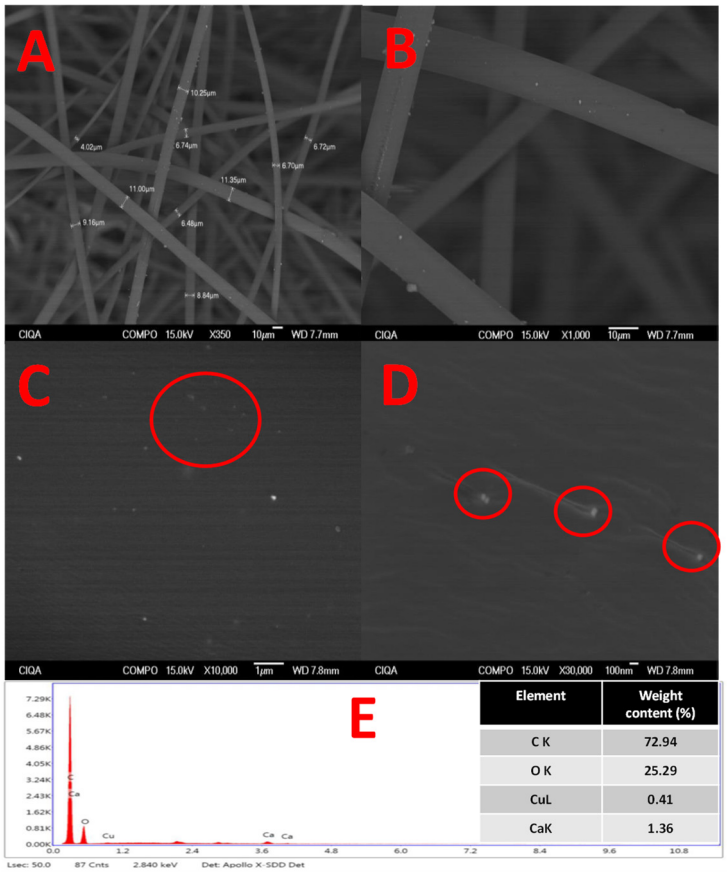

Figure 6. SEM images for the NWF of PET/CuNP (0.5% w/w) sample at different magnifications. A) 350X, B) 1000X, C) 10,000X and D) 30,000X.

3.1.7. Antimicrobial Properties

Multifilaments. Various reports in the literature have shown compelling evidence that metallic nanoparticles, their oxides, and alloys have antimicrobial activity and that this can be maintained when incorporated into a polymer matrix [6,7,27,33,44]. However, in the field of textiles, the addition of these nanoparticles has predominated at a stage subsequent to the manufacturing of the textile itself, mostly through impregnation methods [45,46]. Few reports in the literature have successfully tested the incorporation of nanoparticles in a polymeric matrix capable of being transformed into a textile and verifying that the antimicrobial activity is maintained [13–15].

Figure 7 shows the results obtained for the inhibition of the growth of bacteria *E. coli* (gram-negative) and *S. aureus* (gram-positive) following the procedure described in the Japanese Industrial Standard JIS Z2801 and reported in previous works [27–29]. The antimicrobial activity, indicated as a percentage of inhibition, shows an increase in the ability of the multifilaments with different concentrations of CuNP to inhibit the growth of bacteria in both cases as the content increases, too. It should be noted that *E. coli* turned out to be more susceptible to CuNP from a concentration of 0.25%, showing a reduction in the growth of the microorganism of 90% and close to 99% with a content of 0.5% (w/w) of CuNP. For its part, *S. aureus* presents more excellent resistance when using concentrations of less than 0.25% of CuNP, while with 0.5%, the inhibition percentage is close to 100%.

Preprints (www.preprints.org) | NOT PEER-REVIEWED | Posted: 6 November 2023 doi:10.20944/preprints202311.0279.v1

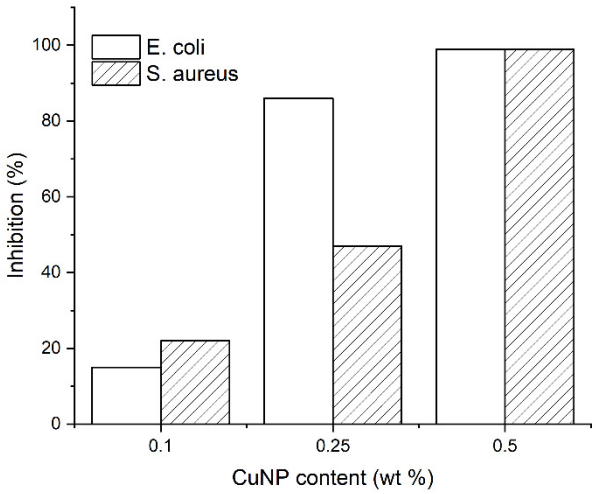

Figure 7. Percentage of inhibition of polyester core/shell multifilaments with different amounts of CuNP against strains of E. coli and S. aureus.

Non-woven fabrics. On the other hand, for NWF samples with different CuNP content, the agar diffusion test was performed to identify the ability to inhibit the growth of pathogenic fungi and bacteria, Figure 8. In the case *C. albicans*, which causes oral candidiasis and is persistent in hospital environments and has the ability to spread rapidly, only when using the highest content of CuNP 0.5% (w/w), no growth is observed in the area covered by the NWF sample. A similar behavior is presented for *S. aureus* when using concentrations of 0.5% (w/w) of CuNP, while for *E. coli*, a total inhibition of bacterial growth is observed throughout the culture medium for all CuNP concentrations used. The above agrees with the results obtained in the tests for core/shell multifilaments, where E. coli showed greater susceptibility to CuNP from a concentration of 0.25% (w/w).

The addition of CuO and CuO@ZrP hybrids to PET matrix and transformation in fibers, using concentrations of 0.1, 0.2, 0.4, and 0.6%, was done by Zhou et al. and tested against *E. coli*, *S. aureus*, and *C. albicans*. Their results showed a microbial reduction >99% for *E. coli* and *S. aureus*; meanwhile, *C. albicans* needs a higher content of 0.6% to obtain a microbial decrease of 97% [13]. As expected, the design of the (textile) fiber has a significant influence on the inhibition of the growth of the microorganisms, since, as shown previously, when the CuNPs are confined to the outside of the filament (forming a shell with a high content of nanoparticles) the possibility of interaction with the cell wall of the microorganism increases and therefore can induce more significant damage, influencing the reproductive cycle. For its part, when the nanoparticles are dispersed throughout the cross-section of the filament, the possibility of interaction with the cell wall decreases, and, therefore, the antimicrobial properties also decrease, at the same concentration. It has also been noted that the structure of the cell walls of gram-positive and gram-negative bacteria plays an important role in susceptibility to various antimicrobial agents, with gram-positive bacteria being more resistant than their gram-negative counterparts [47,48].

Although it was demonstrated that polymeric nanocomposites based on PET/CuNP have antimicrobial and antifungal activity, it is evident that more research is needed on the potential risks of these materials through the evaluation of cytotoxicity and other tests that demonstrate their safe use when in contact with human beings, in personal protective equipment, hospital textiles, filtration devices, etc., [33,49].

Preprints (www.preprints.org) | NOT PEER-REVIEWED | Posted: 6 November 2023 doi:10.20944/preprints202311.0279.v1

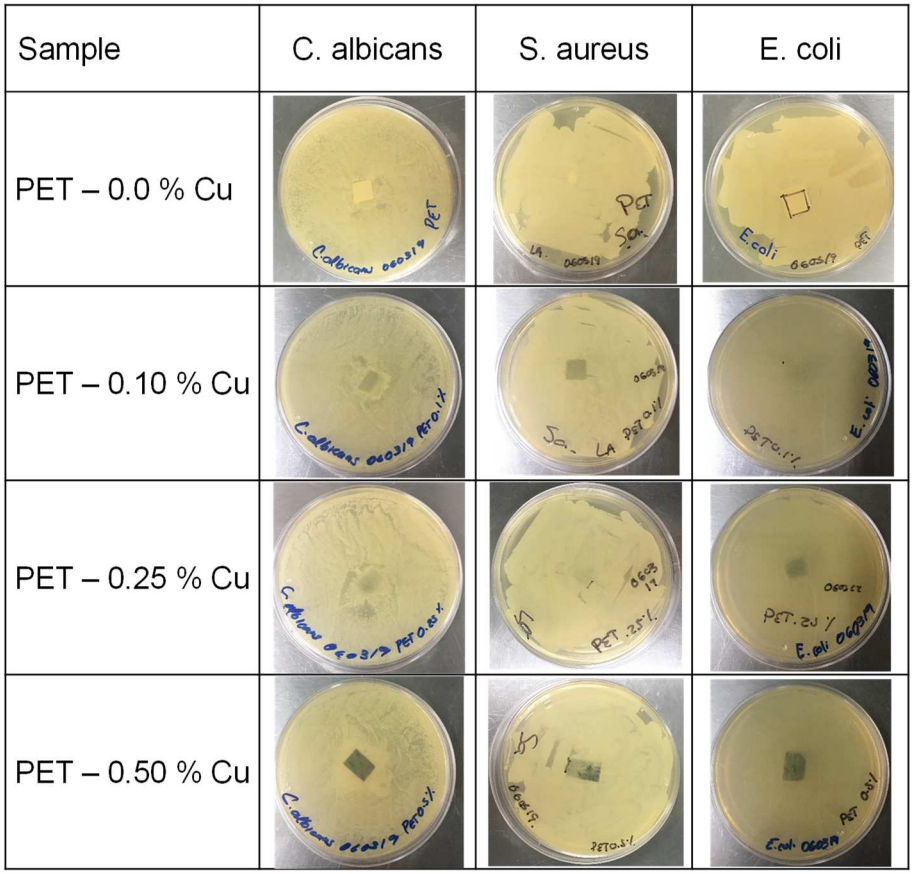

Figure 8. Agar diffusion tests for NWF samples with different CuNP content against *C. albicans*, *S. aureus*, and *E. coli.*

4. Discussion

From the previous results, two fundamental aspects are derived. The first one indicates a close relationship between the size of the copper nanoparticles and their antibacterial properties because the probability of interaction with the cell wall of bacteria increases. This phenomenon occurs due to the adhesion of the fibers and CuNP exposed on the surface with the cell membrane of the *S. aureus* and *E. coli* strains in a way that damages the permeability, as well as the respiration of the bacteria. The inhibition in the growth/reproduction of bacteria is caused by the interaction of CuNP with sulfur-containing compounds, such as DNA, as has been proposed by [29,33]. The other aspect that is important to highlight is the design of the fiber itself [39], since by choosing a configuration of core (inert) and shell (active), the different concentrations of CuNP were confined in the shell of the filament, increasing the possibility interaction with the cell wall of bacteria. The previous results could be very different if the entire cross-section of the filament contained the CuNP since those found inside could not participate directly or come into direct contact with the cell wall of the bacteria, significantly reducing the inhibition of the growth of microorganisms, as shown in the NWF. In order to enhance the antimicrobial activity of NWF, two options arise: a change in fiber cross-section, for example, delta shape, or obtaining bi-component core/shell NWF [37,40].

5. Conclusions

The demand for functional textiles, particularly in the medical and healthcare sector, requires the development of new materials that can efficiently satisfy these needs in an economical, safe, and sustainable manner. By incorporating CuNP into a polyester resin, it was possible to modify its main thermal transitions, particularly the melting and crystallization temperature, without compromising its thermal stability. The above suggested that the nanocomposite is susceptible to be processed by melt-spinning melt-blowing. Filaments with a core/shell configuration and NWF were obtained with

different concentrations of 0.1, 0.25, and 0.5% w/w of CuNP. The denier and grammage increase as the nanoparticle content increase in the samples. Through optical microscopy, it was possible to demonstrate the formation of a core/shell configuration and uniform continuous filaments in the NWF. On the other hand, the presence of CuNPs was evident in the samples in both presentations, showing that the nanoparticles are homogeneously distributed and that some of them are exposed on the surface. Bacterial growth inhibition tests show that *E. coli* is more susceptible than *S. aureus*; when 0.5% CuNP is used in the core/shell multifilament, both bacteria exhibit an inhibition close to 100%, evidencing a bactericidal effect. When an NWF is obtained, the inhibitory effect decreases significantly even against *C. albicans* and *S. aureus*; however, against *E. coli*, the samples have a high capacity to inhibit growth, even when using very low concentrations of CuNP. The design of the (textile) fiber has a significant influence on inhibiting the growth of the microorganism since if the antimicrobial additive is confined to a surface layer of the fiber (core/shell multifilaments) instead of dispersing throughout the cross-section of the fiber (NWF), the antimicrobial effect is increased.

6. Patents

Patent (granted) MX 385261 - 2021.

Author Contributions: Conceptualization, C.A.A.O.; and V.J.C.D.; methodology, F.S.C., and A.S.L.P.; validation, F.S.C.; A.S.L.P. and N.R.F.; formal analysis, A.S.G.; and F.S.C.; investigation, R.R.M.; and J.E.H.B.; resources, J.A.V.G; writing—original draft preparation, A.S.G.; R.R.M.; and J.E.H.B.; writing—review and editing, C.A.A.O.; and V.J.C.D.; visualization, F.S.C.; supervision, F.S.C.; A.S.L.P. and N.R.F.; project administration, J.A.V.G.; and V.J.C.D.; funding acquisition, C.A.A.O. All authors have read and agreed to the published version of the manuscript.

Funding: This research was funded by the consortium project 268003 (MX), 102729 (UK), "Antimicrobial Textiles for the Health Sector" (ACTin,) supported by Innovate UK/CONACYT/Newton Fund. Thanks to the National Council of Humanities, Science and Technology (CONAHCyT) for the scholarship awarded (A.S.G.).

Acknowledgments: Thanks to Maria Guadalupe Mendez, Alfonso Mercado, Carmen Alvarado, and Martha Alicia Fernandez for their technical support.

Conflicts of Interest: The authors declare no conflict of interest. The funders had no role in the design of the study; in the collection, analyses, or interpretation of data; in the writing of the manuscript; or in the decision to publish the results.

References

1. Forrester, J.D.; Maggio, P.M.; Tennakoon, L. Cost of Health Care–Associated Infections in the United States. *J. Patient Saf.* **2022**, *18*, e477–e479, doi:10.1097/PTS.0000000000000845.
2. Wilcox, M.H.; Dryden, M. Update on the Epidemiology of Healthcare-Acquired Bacterial Infections: Focus on Complicated Skin and Skin Structure Infections. *J. Antimicrob. Chemother.* **2021**, *76*, iv2–iv8, doi:10.1093/jac/dkab350.
3. Zimlichman, E.; Henderson, D.; Tamir, O.; Franz, C.; Song, P.; Yamin, C.K.; Keohane, C.; Denham, C.R.; Bates, D.W. Health Care-Associated Infections: AMeta-Analysis of Costs and Financial Impact on the US Health Care System. *JAMA Intern. Med.* **2013**, *173*, 2039–2046, doi:10.1001/jamainternmed.2013.9763.
4. Tanasa, F.; Teaca, C.-A.; Nechifor, M.; Ignat, M.; Duceac, I.A.; Ignat, L. Highly Specialized Textiles with Antimicrobial Functionality—Advances and Challenges. *Textiles* **2023**, *3*, 219–245, doi:10.3390/textiles3020015.
5. Gulati, R.; Sharma, S.; Sharma, R.K. Antimicrobial Textile: Recent Developments and Functional Perspective. *Polym. Bull.* **2022**, *79*, 5747–5771, doi:10.1007/s00289-021-03826-3.
6. Bashari, A.; Shakeri, M.; Shirvan, A.R.; Najafabadi, S.A.N. Functional Finishing of Textiles via Nanomaterials. In *Nanomaterials in the Wet Processing of Textiles*; 2018; pp. 1–70 ISBN 9781119459804.
7. Sowa-Söhle, E.N.; Schwenke, A.; Sajti, C.L.; Wagener, P.; Weiss, A.; Wiegel, H.; Haverich, A. Antimicrobial Efficacy, Cytotoxicity, and Ion Release of Mixed Metal (Ag, Cu, Zn, Mg) Nanoparticle Polymer Composite Implant Material. *BioNanoMaterials* **2013**, *14*, 217–227, doi:10.1515/bnm-2013-0012.
8. Vu, N.N.; Venne, C.; Ladhari, S.; Saidi, A.; Moskovchenko, L.; Lai, T.T.; Xiao, Y.; Barnabe, S.; Barbeau, B.; Nguyen-Tri, P. Rapid Assessment of Biological Activity of Ag-Based Antiviral Coatings for the Treatment

of Textile Fabrics Used in Protective Equipment Against Coronavirus. *ACS Appl. Bio Mater.* **2022**, *5*, 3405–3417, doi:10.1021/acsabm.2c00360.

9. Parham, S.; Kharazi, A.Z.; Bakhsheshi-Rad, H.R.; Kharaziha, M.; Ismail, A.F.; Sharif, S.; Razzaghi, M.; RamaKrishna, S.; Berto, F. Antimicrobial Synthetic and Natural Polymeric Nanofibers as Wound Dressing: A Review. *Adv. Eng. Mater.* **2022**, *24*, doi:10.1002/adem.202101460.
10. Su, X.; Sha, Q.; Gao, X.; Li, J.; Wu, Y.; Li, W.; Wu, W.; Han, N.; Zhang, X. Lightweight, Multifunctional Smart MXene@PET Non-Woven with Electric/Photothermal Conversion, Antibacterial and Flame Retardant Properties. *Appl. Surf. Sci.* **2023**, *639*, doi:10.1016/j.apsusc.2023.158205.
11. Saylor, Y.; Irby, V. *Metal Nanoparticles: Properties, Synthesis and Applications*; 2018; ISBN 9781536141160.
12. Ren, G.; Hu, D.; Cheng, E.W.C.; Vargas-Reus, M.A.; Reip, P.; Allaker, R.P. Characterisation of Copper Oxide Nanoparticles for Antimicrobial Applications. *Int. J. Antimicrob. Agents* **2009**, *33*, 587–590, doi:10.1016/j.ijantimicag.2008.12.004.
13. Zhou, J.; Fei, X.; Li, C.; Yu, S.; Hu, Z.; Xiang, H.; Sun, B.; Zhu, M. Integrating Nano-Cu 2 O@ZrP into in Situ Polymerized Polyethylene Terephthalate (PET) Fibers with Enhanced Mechanical Properties and Antibacterial Activities. *Polymers (Basel).* **2019**, *11*, doi:10.3390/polym11010113.
14. Zhu, Y.; Wang, Y.; Sha, L.; Zhao, J. Preparation of Antimicrobial Fabric Using Magnesium-Based PET Masterbatch. *Appl. Surf. Sci.* **2017**, *425*, 1101–1110, doi:10.1016/j.apsusc.2017.07.044.
15. Yeo, S.Y.; Jeong, S.H. Preparation and Characterization of Polypropylene/Silver Nanocomposite Fibers. *Polym. Int.* **2003**, *52*, 1053–1057, doi:10.1002/pi.1215.
16. Guerra, M.A.; Mariano, N.A.; Ramos, A.S.; Campos, M.G.N. Processing of Pet-Silver Nanocomposite Filaments. In Proceedings of the Materials Science Forum; 2016; Vol. 869, pp. 350–355.
17. Guzman, A.; Cárcamo, H.; León, O. Elaboración y Caracterización Estructural de Fibras de Tereftalato de Polietileno (PET) Dopadas Con Nanocobre (0) Utilizando Proceso de Extrusión. *Rev. Peru. Química e Ing. Química* **2014**, *17*, 9–13.
18. Abazari, M.; Badeleh, S.M.; Khaleghi, F.; Saeedi, M.; Haghi, F. Fabrication of Silver Nanoparticles-Deposited Fabrics as a Potential Candidate for the Development of Reusable Facemasks and Evaluation of Their Performance. *Sci. Rep.* **2023**, *13*, doi:10.1038/s41598-023-28858-9.
19. Ferreira, T.; Vale, A.C.; Pinto, A.C.; Costa, R. V.; Pais, V.; Sousa, D.; Gomes, F.; Pinto, G.; Dias, J.G.; Moreira, I.P.; et al. Comparison of Zinc Oxide Nanoparticle Integration into Non-Woven Fabrics Using Different Functionalisation Methods for Prospective Application as Active Facemasks. *Polymers (Basel).* **2023**, *15*, doi:10.3390/polym15173499.
20. Chruściel, J.J.; Olczyk, J.; Kudzin, M.H.; Kaczmarek, P.; Król, P.; Tarzyńska, N. Antibacterial and Antifungal Properties of Polyester, Polylactide, and Cotton Nonwovens and Fabrics, by Means of Stable Aqueous Dispersions Containing Copper Silicate and Some Metal Oxides. *Materials (Basel).* **2023**, *16*, 417–427, doi:10.3390/ma16165647.
21. Gabbay, J.; Borkow, G.; Mishal, J.; Magen, E.; Zatcoff, R.; Shemer-Avni, Y. Copper Oxide Impregnated Textiles with Potent Biocidal Activities. *J. Ind. Text.* **2006**, *35*, 323–335, doi:10.1177/1528083706060785.
22. Ávila-Orta, C.A.; Quiñones-Jurado, Z. V.; Waldo-Mendoza, M.A.; Rivera-Paz, E.A.; Cruz-Delgado, V.J.; Mata-Padilla, J.M.; González-Morones, P.; Ziolo, R.F. Ultrasound-Assist Extrusion Methods for the Fabrication of Polymer Nanocomposites Based on Polypropylene/Multi-Wall Carbon Nanotubes. *Materials (Basel).* **2015**, *8*, 7900–7912, doi:10.3390/ma8115431.
23. A. Ávila-Orta, C.; González-Morones, P.; Agüero- Valdez, D.; González-Sánchez, A.; G. Martínez-Colunga, J.; M. Mata-Padilla, J.; J. Cruz-Delgado, V. Ultrasound-Assisted Melt Extrusion of Polymer Nanocomposites. In *Nanocomposites - Recent Evolutions*; Sivasankaran, S., Ed.; IntechOpen: London, 2019; Vol. 1.
24. J. Cruz-Delgado, V.; A. Valdez-Garza, J.; M. Mata-Padilla, J.; G. Martínez-Colunga, J.; A. Ávila-Orta, C. Preparation and Characterization of Electrically Conductive Polymer Nanocomposites with Different Carbon Nanoparticles. In *Carbon Nanotubes - Redefining the World of Electronics*; IntechOpen, 2021; pp. 11–28.
25. Andrade-Guel, M.; Reyes-Rodríguez, P.Y.; Cabello-Alvarado, C.J.; Cadenas-Pliego, G.; Ávila-Orta, C.A. Influence of Modified Carbon Black on Nylon 6 Nonwoven Fabric and Performance as Adsorbent Material. *Nanomaterials* 2022, *12*.
26. Cabello-Alvarado, C.; Andrade-Guel, M.; Medellin-Banda, D.I.; Ávila-Orta, C.A.; Cadenas-Pliego, G.; Sáenz-Galindo, A.; Radillo-Radillo, R.; Lara-Sánchez, J.F.; Melo-Lopez, L. Non-Woven Fabrics Based on

Nylon 6/Carbon Black-Graphene Nanoplatelets Obtained by Melt-Blowing for Adsorption of Urea, Uric Acid and Creatinine. *Mater. Lett.* **2022**, *320*, 132382, doi:https://doi.org/10.1016/j.matlet.2022.132382.

27. España-Sánchez, B.L.; Ávila-Orta, C.A.; Padilla-Vaca, F.; Neira-Velázquez, M.G.; González-Morones, P.; Rodríguez-González, J.A.; Hernández-Hernández, E.; Rangel-Serrano, Á.; Barriga-C., E.D.; Yate, L.; et al. Enhanced Antibacterial Activity of Melt Processed Poly(Propylene) Ag and Cu Nanocomposites by Argon Plasma Treatment. *Plasma Process. Polym.* **2014**, *11*, 353–365, doi:10.1002/ppap.201300152.
28. Espana-Sanchez, B.L.; Avila-Orta, C.A.; Padilla-Vaca, L.F.; Barriga-Castro, E.D.; Soriano-Corral, F.; Gonzalez-Morones, P.; Ramirez-Wong, D.G.; Luna-Barcenas, G. Early Stages of Antibacterial Damage of Metallic Nanoparticles by TEM and STEM-HAADF. *Curr. Nanosci.* **2017**, *14*, 54–61, doi:10.2174/2468187307666170906150731.
29. Navarro-Rosales, M.; Ávila-Orta, C.A.; Neira-Velázquez, M.G.; Ortega-Ortiz, H.; Hernández-Hernández, E.; Solís-Rosales, S.G.; España-Sánchez, B.L.; Gõnzalez-Morones, P.; Jímenez-Barrera, R.M.; Sánchez-Valdes, S.; et al. Effect of Plasma Modification of Copper Nanoparticles on Their Antibacterial Properties. *Plasma Process. Polym.* **2014**, *11*, 685–693, doi:10.1002/ppap.201400013.
30. Mata-Padilla, J.M.; Ávila-Orta, C.A.; Almendárez-Camarillo, A.; Martínez-Colunga, J.G.; Hernández-Hernández, E.; Cruz-Delgado, V.J.; González-Morones, P.; Solís-Rosales, S.G.; González-Calderón, J.A. Non-Isothermal Crystallization Behavior of Isotactic Polypropylene/Copper Nanocomposites. *J. Therm. Anal. Calorim.* **2020**, doi:10.1007/s10973-020-09512-2.
31. Tamayo, L.; Palza, H.; Bejarano, J.; Zapata, P.A. Polymer Composites With Metal Nanoparticles: Synthesis, Properties, and Applications. Synthesis, Properties, and Applications. In *Polymer Composites with Functionalized Nanoparticles: Synthesis, Properties, and Applications*; 2018; pp. 249–286 ISBN 9780128140659.
32. Demchenko, V.; Riabov, S.; Rybalchenko, N.; Shtompel', V. Structure, Morphology, and Properties of Copper-Containing Polymer Nanocomposites. In Proceedings of the Springer Proceedings in Physics; 2017; Vol. 195, pp. 641–659.
33. Tamayo, L.; Azócar, M.; Kogan, M.; Riveros, A.; Páez, M. Copper-Polymer Nanocomposites: An Excellent and Cost-Effective Biocide for Use on Antibacterial Surfaces. *Mater. Sci. Eng. C* 2016, *69*, 1391–1409.
34. León-Martínez, P.A. De; Soriano-Corral, F.; Ávila-Orta, C.A.; González-Morones, P.; Hernández-Hernández, E.; Ledezma-Pérez, A.S.; Covarrubias-Gordillo, C.A.; Espinosa-López, A.C.; Gómez, R.E.D. de L. Surface Modification of $NTiO_2$/Ag Hybrid Nanoparticles Using Microwave-Assisted Polymerization in the Presence of Bis(2-Hydroxyethyl) Terephthalate. *J. Nanomater.* **2017**, *2017*, 7079497, doi:10.1155/2017/7079497.
35. Vassiliou, A.A.; Chrissafis, K.; Bikiaris, D.N. In Situ Prepared PET Nanocomposites: Effect of Organically Modified Montmorillonite and Fumed Silica Nanoparticles on PET Physical Properties and Thermal Degradation Kinetics. *Thermochim. Acta* **2010**, *500*, 21–29, doi:10.1016/j.tca.2009.12.005.
36. Peng, N.; Widjojo, N.; Sukitpaneenit, P.; Teoh, M.M.; Lipscomb, G.G.; Chung, T.-S.; Lai, J.-Y. Evolution of Polymeric Hollow Fibers as Sustainable Technologies: Past, Present, and Future. *Prog. Polym. Sci.* **2012**, *37*, 1401–1424, doi:https://doi.org/10.1016/j.progpolymsci.2012.01.001.
37. Karaca, E.; Ozcelik, F. Influence of the Cross-Sectional Shape on the Structure and Properties of Polyester Fibers. *J. Appl. Polym. Sci.* **2007**, *103*, 2615–2621, doi:10.1002/app.25350.
38. Huuhilo, T.; Nystrom, M. Fouling of a Polypropylene Filter Fabric with Silica. *Filtr. Sep.* **2001**, *38*, 43–47.
39. Naeimirad, M.; Zadhoush, A.; Kotek, R.; Esmaeely Neisiany, R.; Nouri Khorasani, S.; Ramakrishna, S. Recent Advances in Core/Shell Bicomponent Fibers and Nanofibers: A Review. *J. Appl. Polym. Sci.* **2018**, *135*, 46265, doi:https://doi.org/10.1002/app.46265.
40. Lim, J.C.; Park, Y.W.; Kim, H.C. Study on Manufacturing PCT/PPS Flame Retardant Fiber by Sheath/Core Conjugate Spinning. *Fibers Polym.* **2020**, *21*, 498–504, doi:10.1007/s12221-020-9082-x.
41. Kara, S.; Ureyen, M.E.; Erdogan, U.H. Structural and Antibacterial Properties of PP/CuO Composite Filaments Having Different Cross Sectional Shapes. *Int. Polym. Process.* **2016**, *31*, 398–409, doi:10.3139/217.3159.
42. Xue, B.; Jiang, Y.; Liu, D. Preparation and Characterization of a Novel Anticorrosion Material: Cu/LLDPE Nanocomposites. *Mater. Trans.* **2011**, *52*, 96–101, doi:10.2320/matertrans.M2010280.
43. Qufu Wei; Yu, L.; Ning Wu; Shanhu Hong Preparation and Characterization of Copper Nanocomposite Textiles. *J. Ind. Text.* **2008**, *37*, 275–283, doi:10.1177/1528083707083794.
44. Fernandez, A.; Lloret, E.; Llorens, A.; Picouet, P. Metal-Based Micro and Nano-Composites as Antimicrobials in Food Packaging. In *Food Packaging: Procedures, Management and Trends*; 2012; pp. 79–92

ISBN 9781622573103.

45. Ghosh, S.; Sarkar, B.; Thongmee, S.; Mostafavi, E. Hybrid Antibacterial, Antifungal, and Antiviral Smart Coatings. In *Antiviral and Antimicrobial Smart Coatings: Fundamentals and Applications*; 2023; pp. 431–452 ISBN 9780323992916.
46. Odintsova, O.I.; Vladimirtseva, E.L.; Kozlova, O. V.; Smirnova, S. V.; Lipina, A.A.; Petrova, L.S.; Erzunov, K.A.; Konstantinova, Z.A.; Zimnurov, A.R.; Bykov, F.A.; et al. FINISHING TEXTILE MATERIALS WITH MICROCAPSULES AND NANOPARTICLES OF FUNCTIONAL SUBSTANCES. *ChemChemTech* **2023**, *66*, 173–184, doi:10.6060/ivkkt.20236607.6844j.
47. Pardi, G. "Determinantes de Patogenicidad de Candida Albicans" *Acta Odontol. Venez.* **2002**, *40*, 185–192.
48. Dong, X.; Wang, S.; Ren, K. Application of Composite Antibacterial Nanoparticle Non-Woven Fabric in Sterilization of Hospital Infection. *Prev. Med. (Baltim).* **2023**, *173*, doi:10.1016/j.ypmed.2023.107597.
49. García, A.; Rodríguez, B.; Giraldo, H.; Quintero, Y.; Quezada, R.; Hassan, N.; Estay, H. Copper-Modified Polymeric Membranes for Water Treatment: A Comprehensive Review. *Membranes (Basel).* 2021, *11*, 1–47.